

# Metamaterials and FDTD based Numerical Modeling Studies

Sibel Gündüz<sup>1</sup>, Mustafa Çakır<sup>1</sup>, Gonca Çakır<sup>1</sup>, Levent Sevgi<sup>2</sup>

<sup>1</sup>Kocaeli University, Electronics and Communication Engineering Department,

<sup>2</sup>Doğuş University, Electronics and Communication Engineering Department,  
Zeamet Sok. No.21, Acıbadem/Kadıköy, İstanbul, Turkey

*Keywords: Dispersive medium, metamaterials, double negative index materials, left-handed materials, Lorentz model, Drude model, Debye model, wave propagation, FDTD, numerical simulation.*

## ABSTRACT

**Metamaterials (MTM) have attracted great attention for the last couple of years. These new materials have a wide potential range of applications and research has focused on understanding electromagnetic properties of MTM. This presentation aims to review numerical simulation strategies of modeling MTM based on FDTD method and to give characteristic examples.**

Efficient and accurate dispersive MTM-FDTD algorithms have been developed and used to investigate electromagnetic wave interaction with MTMs. This presentation aims to review numerical modeling of MTMs. In particular, a two-dimensional (2D) MTM-FDTD algorithm is developed for this purpose and the time-domain electromagnetic wave interaction with MTMs is investigated.

## I. INTRODUCTION

Materials having negative real parts of both their permittivity and permeability are among popular research topics [1-18]. They are called metamaterials (MTM), left-handed materials (LHM), or double-negative-index materials (DNG). Recent research has focused both on the behavior of these MTMs as well as on the incorporation of negative permittivity and permeability into electromagnetic theory. Electromagnetic properties of MTMs are said to be difficult or impossible to achieve with conventional, naturally occurring materials [1].

Veselago investigated the key theoretical aspects and some applications of MTMs a few decades ago [2]. He pointed out that MTMs have simultaneously negative permittivity and permeability and some unique properties, such as inverse Snell effect, an inverse Doppler shift, and backward-directed Cherenkov radiation [3]. In 1999, Pendry showed that materials with an array of split ring resonators (SRRs) produce negative permeability over certain frequency bands [4]. Combining SRRs with arrays of metallic wires enabled the construction of MTMs with both effective permittivity and permeability negative. Smith in 2001 demonstrated for the first time the experimental existence of MTMs [5]. Since then, numerical modeling, experimental verification, and design studies have increasingly appeared in the literature (see [6] for the most recent comprehensive review of, and [7-10] for interesting discussions on, MTMs).

Numerical MTM modeling studies are mostly based on the finite-difference time-domain (FDTD) method.

## II. METAMATERIALS

Electromagnetic response of a system is determined to a large extent by the electrical properties of the materials involved. These macroscopic parameters are the permittivity  $\epsilon$ , permeability  $\mu$ , and conductivity  $\sigma$ . A medium with both permittivity and permeability greater than zero ( $\epsilon > 0$ ,  $\mu > 0$ ) is called a double positive (DPS) medium. A medium with permittivity less than zero and permeability greater than zero ( $\epsilon < 0$ ,  $\mu > 0$ ) is designated as  $\epsilon$ -negative (ENG) medium. Many plasmas exhibit this characteristic in certain frequency regimes. A medium with the permittivity greater than zero and permeability less than zero ( $\epsilon > 0$ ,  $\mu < 0$ ) is called a  $\mu$ -negative (MNG) medium. Some gyrotropic materials exhibit this characteristic in certain frequency regimes. Finally, materials with permittivity and permeability both less than zero ( $\epsilon < 0$ ,  $\mu < 0$ ) are called double-negative (DNG) media.

One of the main reasons researchers have investigated MTMs is the possibility to create a structure with a negative refractive index, since this property is not found in any naturally occurring material. Almost all materials encountered in optics, such as glass or water, have positive values for both  $\epsilon$  and  $\mu$ . However, many metals (such as silver and gold) have negative  $\epsilon$  at visible wavelengths. Materials with either  $\epsilon$  or  $\mu$  (but not both) negative are opaque to electromagnetic radiation.

Although the optical properties of a transparent material are fully specified by the parameters  $\epsilon$  and  $\mu$ , in practice the refractive index  $n = \pm\sqrt{\epsilon_r\mu_r}$  is often used. All known

transparent materials possess positive values for  $\epsilon$  and  $\mu$ . By convention the positive square root is used for  $n$ . However, some engineered MTMs have  $\epsilon < 0$  and  $\mu < 0$ ; under such circumstances, the negative square root is taken for  $n$  ( $n = \sqrt{(-\epsilon_r)(-\mu_r)} = \sqrt{e^{j\pi} \epsilon_r e^{j\pi} \mu_r}$  which yields  $n = -\sqrt{\epsilon_r \mu_r}$ ). For the MTMs with negative  $n$  Snell's law ( $n_1 \sin \theta_1 = n_2 \sin \theta_2$ ) still applies, but as  $n_2$  is negative, the rays will be refracted on the *same* side of the normal on entering the MTM. Moreover, the Doppler shift is reversed: meaning that the frequency of a light source moving toward an observer appears to reduce. Finally, the time-averaged Poynting vector is anti-parallel to phase velocity; i.e., the wave fronts are moving in the opposite direction to the flow of energy. For a plane wave propagating in the MTM, the electric field, magnetic field and Poynting vector follow a left-hand rule, thus giving rise to the name LHM materials. These are illustrated in Fig. 1.

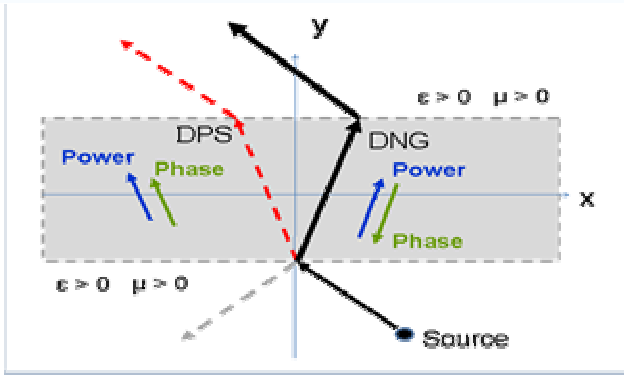


**Figure 1:** Wave propagation through DPS and DNG media, and reflections and refractions

In reality, all material properties are frequency-dependent. There are several models that have been constructed to describe the frequency response of materials. Electrical susceptibility (hence, permittivity) and magnetic susceptibility (hence, permeability) are used in these models. Maxwell equations are standard

$$\frac{\partial}{\partial t} \vec{D} = \vec{\nabla} \times \vec{H}, \quad \frac{\partial}{\partial t} \vec{B} = -\vec{\nabla} \times \vec{E} \quad (1)$$

But, constitutive relations in the frequency domain for dispersive materials are given as

$$D(\omega) = \epsilon_0 [\epsilon_\infty + \chi_e(\omega)] E(\omega) \quad (2)$$

$$B(\omega) = \mu_0 [\mu_\infty + \chi_m(\omega)] H(\omega). \quad (3)$$

Here,  $\chi_e(\omega)$  and  $\chi_m(\omega)$  are electric and magnetic susceptibilities, respectively, and,  $\epsilon_\infty$ ,  $\mu_\infty$  correspond to high frequency limiting (optical) values. Frequency-dependent complex permittivity and permeability are then defined as

$$\epsilon(\omega) = \epsilon_0 (\epsilon_\infty + \chi_e(\omega)). \quad (4a)$$

$$\mu(\omega) = \mu_0 (\mu_\infty + \chi_m(\omega)). \quad (4b)$$

Temporal responses may be obtained once the frequency domain representations are specified.

### LORENTZ MODEL

The Lorentz model describes the polarization (electric dipole) – electric field relation  $P = \epsilon_0 \chi_e(\omega) E$ . These are given in both domains as

$$P(\omega) = \frac{g_L}{-\omega^2 + j\delta_L \omega + \omega_k^2} \epsilon_0 E(\omega) \quad (5)$$

$$\frac{d^2}{dt^2} P + \delta_L \frac{d}{dt} P + \omega_k^2 P = \epsilon_0 g_L E. \quad (6)$$

The first term on the left of (6) is for the acceleration of the charges, the second is for the damping mechanisms of the system with damping coefficient  $\delta_L$  and the third is for the restoring forces with the plasma (resonance) frequency  $\omega_k$ . On the right side of the equation the term exhibits a coupling coefficient  $g_L$ .

### DEBYE MODEL

If the acceleration term (i.e., the first term in (6)) is small compared to the others in Lorentz model and is neglected Debye model is obtained:

$$\chi_{eD}(\omega) = \frac{g_D}{j\delta_D \omega + \omega_k^2}. \quad (7)$$

### DRUDE MODEL

Neglecting the restoring force (i.e., the third term in (6) in Lorentz model yields the Drude model:

$$\chi_{eDr}(\omega) = \frac{g_{Dr}}{-\omega^2 + j\delta_{Dr} \omega}. \quad (8)$$

In all these models, the high-frequency limit reduces the permittivity to that of free space. Only Lorentz and the Drude models can produce negative permittivities or permeabilities when the coupling coefficient is positive. Because the Lorentz model is resonant, the real part of the susceptibility and, hence, that of the permittivity become negative in a narrow frequency region immediately above the resonance. On the other hand, the Drude model can yield a negative real part of the permittivity.

Complex relative permittivity has frequency dependent real and imaginary parts, where the real part characterizes the refractive property, while the imaginary one characterizes the absorptive property of material. As an example, real and imaginary parts of a Lorentz material vs. frequency are plotted in Fig. 2. The shaded region is the region of anomalous dispersion. The real part of permittivity decreases with increasing frequency in this region; causing an increase in the group velocity. The imaginary part of the permittivity makes a peak in the anomalous dispersion region, indicating that the material present a high attenuation to signal frequencies present in

this region. The regions outside the anomalous region is said to have a normal dispersion.

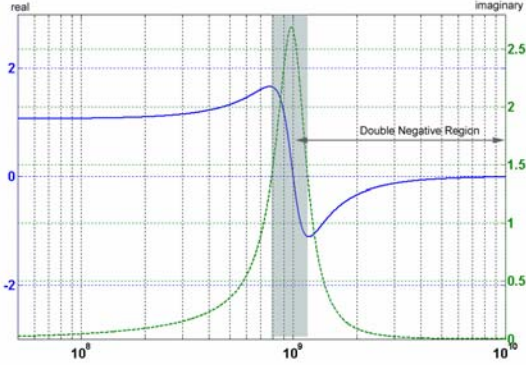


**Figure 2:** Real and Imaginary part of Lorentz material. The real part of relative permittivity of lossy MTM has negative value above 1 GHz to 7 GHz. Thus double negative regions appears from 1 GHz to 7 GHz ( $\epsilon_k = 2e14 - 2$ ,  $\alpha_k = 1$ ,  $\delta_k = 0.2$ ,  $\omega_k = 1e9 \times (1e - 7)$ ).

A generic form of the electric susceptibility is given as

$$\chi_e = \sum_k \frac{\epsilon_k}{\alpha_k + i \cdot 2 \cdot \delta_k \left( \frac{\omega}{\omega_k} \right) - \left( \frac{\omega}{\omega_k} \right)^2} \quad (10)$$

This equation lets to define an arbitrary number of media using an arbitrary number of resonances per medium. An example for  $k=3$  (dual plasma resonance) is pictured in Fig. 3. Values used in this example are listed in Table 1.

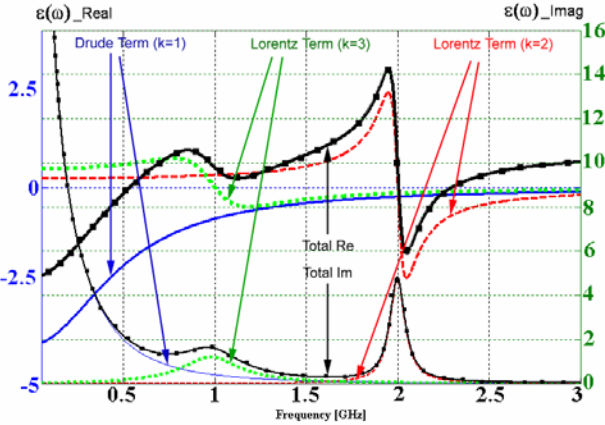


**Figure 3:** A dispersive medium with double plasma resonances around 1GHz and 2GHz.

### III. FDTD METHOD IN DISPERSIVE MEDIA

Originally the FDTD scheme (Yee's algorithm [11]) was proposed with the assumption that the medium was non-dispersive; constitutive parameters of permittivity and permeability are constant. In reality, these parameters vary with frequency; such as water, biological tissues, and MTMs discussed here. Several techniques have been proposed in order to incorporate frequency dispersion into the FDTD codes [12,18].

**Table 1:** Numerical values used for Figure 2.

	k=1	k=2	k=3
$\alpha_k$	0	1	1
$\delta_k$	0.25	0.025	0.2
$\omega_k$	1GHz	2GHz	1GHz
$\epsilon_k$	1	0.236	0.473

The well-known standard Yee time-stepping iterative equations need to be modified in order to model a dispersive medium. Several dispersive FDTD methods, such as Recursive Convolution (RC), Auxiliary Differential Equation (ADE) and Z-transform (ZT) methods have been used. ADE method was proposed by Kashiwa and co-workers [15]. Here, the constitutive relation between electric flux density and electric field is expressed by an ordinary equation in the time domain by utilizing the inverse Fourier transformation. In the RC approach, this is achieved directly in the time domain through a convolution integral [17]. Again, the relation between  $D$  and  $E$  is used in the ZT approach. This is first implemented in the FDTD method by Sullivan [18].

ADE method is used here and a 2D TE-type MTM-FDTD code is developed. It should be noted that the terms TE and TM are used differently in electromagnetic and optics societies. TE and TM stand for transverse electric and transverse magnetic, respectively. These terms are used for guided wave propagation problems, which are best solved by decomposing wave equations and wave fields into transverse and longitudinal components. The longitudinal direction is the direction of guided propagation. In electromagnetics it is customary to assume z-axis as the longitudinal direction, and the xy-plane as the transverse plane. Therefore, TEz-type and TMz-type 2D problems mean  $E_z = 0$  and  $H_z = 0$ , respectively. The corresponding field components for the TEz and TMz type problems are  $H_x, E_y, H_z$  and  $E_x, H_y, H_z$ , respectively. Under this terminology, for example, a 2D MTM-Slab may be assumed infinite-extend along y-direction and is located on the xz-plane.

In recent FDTD-based MTM modeling studies the 2D MTM-Slab is located on xy-plane and is assumed infinite along z-direction. Under this assumption, the field components for the TE-type problem are specified to be  $E_x, E_y$ , and  $H_z$ . This is given in Fig. 4. The same structure and the latter terminology are also used in this presentation. The flow chart of both standard-FDTD and MTM-FDTD algorithms are given in Fig. 5. As shown, electric displacement  $D$  values are updated using  $H$  fields, while magnetic flux  $B$  values are updated from  $E$  fields. This is achieved via updating electric and magnetic polarizations.

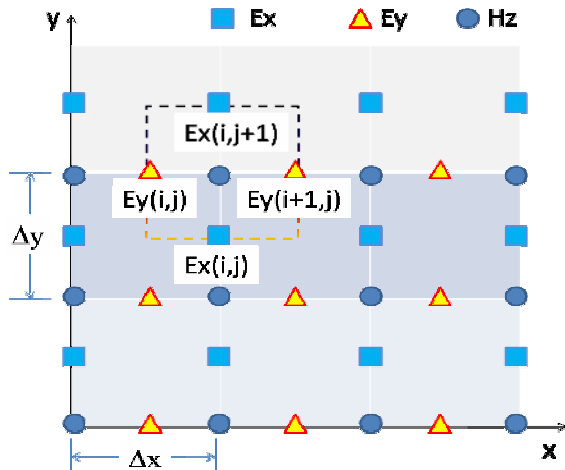


Figure 4: The 2D TE-type FDTD space

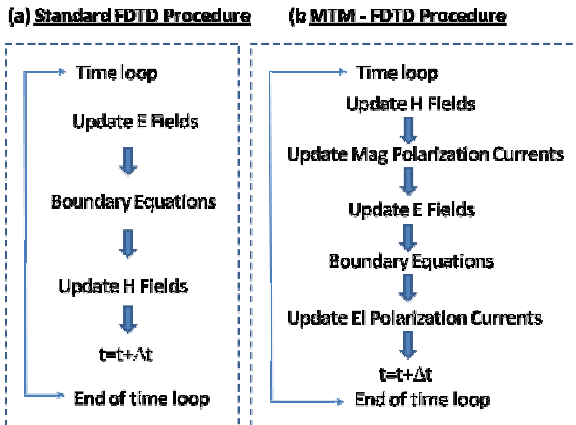


Figure 5: Flow charts of (a) Standard-FDTD, (b) MTM-FDTD algorithms

#### IV. A 2D MTM SLAB and FDTD SIMULATIONS

A finite-length, infinite-extend MTM slab has been extensively used for the visualizations of electromagnetic wave – MTM interactions [7-10]. As summarized in Sec. II, waves hitting MTM layer boundary will be refracted on the *same* side of the normal and wave fronts are moving in the opposite direction of energy flow. This will be illustrated in this Section using MTM-FDTD.

An infinite-extend MTM layer having finite thickness is located on the  $xy$ -plane as shown in Fig. 1. The parameters are chosen in such a way that around 1GHz operating frequency the imaginary part of the MTM slab permittivity and permeability become negligible and real parts are approximately equal to -1. The frequency range where the relative permittivity and permeability are sufficiently close to -1 is very narrow. Thus, the time dependence of the excitation must be specified in such a way that its spectrum is very narrow. This necessitates the use of smoothly ramped sinusoidal signals (e.g., see equation (12) in [8]). A steady state regime is reached after a long simulation times because of the slow convergence.

Fig. 6 shows frequency variations of relative permittivity and permeability for the set of parameters listed in Table 1. The imaginary part is approximately zero. All parameters of electrical and magnetic susceptibilities are chosen the same, so curves belong both of them. Two curves correspond to two sets of parameters; giving  $n = -1$  at the plasma frequencies of 1 GHz and 1.2 GHz, respectively.

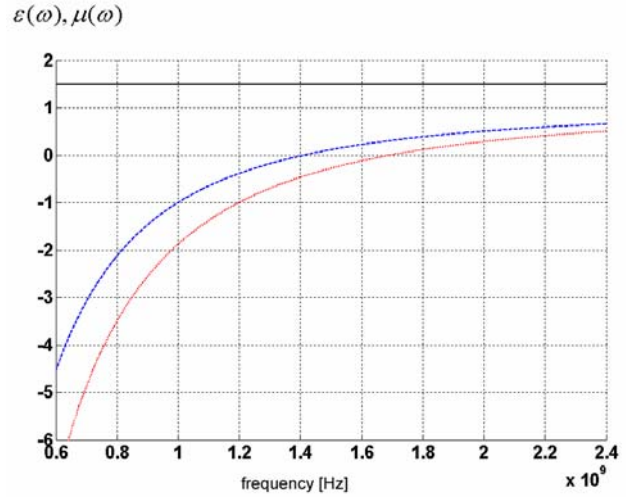


Figure 6: Permittivity and permeability of the MTM-Slab

The first simulation result is given in Fig. 7 for a lossless DPS slab. Here, standard FDTD is used. The 2D FDTD space is  $701 \times 351$ ,  $\Delta x = \Delta y = 1$  mm,  $f = 1$  GHz (i.e.,  $\lambda = 30$  cm), slab thickness  $d = 1$  mm ( $= \lambda/30$ ),  $\Delta t = 0.02 / f = 20$  ps. Source is injected via  $E_x$ -field 0.5 mm away from the DPS layer.

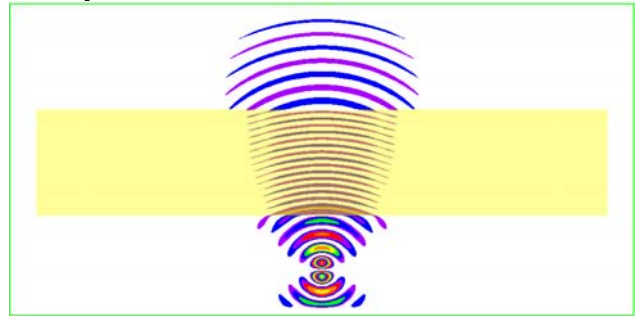
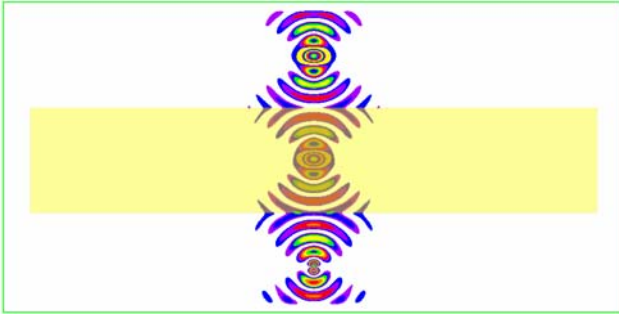


Figure 7: Propagation through a DPS dielectric slab with  $\epsilon_r = 1.5$  and  $\mu_r = 1$  (normal incidence).

The simulations with the same operational parameters are repeated for the DNG (MTM) layer; the results are plotted in Fig. 8. As shown from Fig. 6, both relative permittivity and permeability at 1 GHz is -1. Therefore, there is a perfect match at the DPS – DNG boundary. The foci occur at equal distance.



**Figure 8:** Propagation through a MTM-Slab ( $f=1$  GHz and  $n = -1$  ).

The last simulation result is given in Fig. 9 and belongs to a case where both relative permittivity and permeability at 1 GHz is around -2. Therefore, the focal distance is twice the distance between source and DPS-DNG boundary.

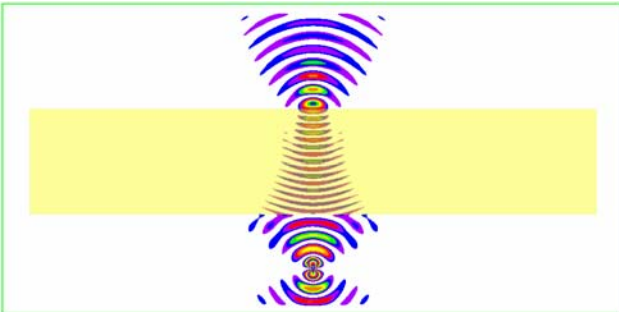


**Figure 9:** Propagation through a MTM-Slab ( $f=1$  GHz and  $n = -2$  ).

## V. CONCLUSION

In this presentation, numerical modeling and simulation studies on metamaterials are reviewed. Two-dimensional FDTD-Based algorithms of both TE<sub>z</sub> and TM<sub>z</sub> type problems are developed. Electromagnetic wave – metamaterial slab interactions are investigated. Wave propagation through the boundary of double positive medium – double negative medium is visualized.

## REFERENCES

1. J. A. Kong, "Electromagnetic wave interaction with stratified negative isotropic media," *J. Electromagnetic Waves and Applications*, Vol. 15, No. 10, 2001.
2. V. G. Veselago, "The electrodynamics of substances with simultaneously negative values of permittivity and permeability," *Soviet Physics*, Vol. 10, No. 4, January 1968.
3. L. Lu, Characterization and Application of Left-Handed Meta-materials Using the Dispersive Finite-Difference Time-Domain Method, PhD Dissertation, May 2006.
4. J. B. Pendry, A. J. Holden, W. J. Stewart, and I. Youngs, "Extremely low frequency plasmons in metallic mesostructures," *IEEE Trans. on MTT*, vol. 47, pp. 2075-2084, 1999.
5. D. R. Smith, W. J. Padilla, D. C. Vier, S. C. Nemat-Nasser, and S. Schultz, "Composite media with simultaneously negative permeability and permittivity," *Physical Review Letters*, vol. 84, pp. 4184-4187, 2001.
6. V. Veselago, L. Braginsky, V. Shklover, C. Hafner, "Negative Rectactive Index Materials," *J. Computational and Theoretical Nanoscience*, Vol. 3, No.2, pp.1-30, 2006
7. R. W. Ziolkowski, A. D. Kipple, "Causality and double-negative Metamaterials," *Physical Review*, Vol. 68, 26615, pp.1-9, 2003.
8. R. W. Ziolkowski, "Pulsed and Gaussian Beam Interactions with Double Negative Metamaterial Slabs," *Optics Express*, Vol. 11, No. 7, pp.662-680, 2003.
9. J. B. Brock, A. A. Houck, I. Chuang, "Focusing Inside Negative Index Materials," *Applied Physics Lett.*, Vol. 85, No.13, pp.2472-2474, 2004.
10. S. Foteinopoulou, E. N. Economou, C. M. Soukoulis, "Refraction in Media with a Negative Refractive Index," *Physical Review Lett.*, Vol. 90, No.10, 107402, pp. 1-4, 2003.
11. K. S. Yee, "Numerical solution of initial boundary value problems involving Maxwell's equations in isotropic media," *IEEE Trans. on AP*, Vol. AP-14, pp. 302-307, May 1966.
12. R. J. Luebbers, F. Hunsberger, K. S. Kunz, R. B. Standler, M. Schneider, "A frequency-dependent finite-difference time-domain formulation for dispersive materials," *IEEE Trans. on EMC*, Vol. 32, pp. 222-227, Aug. 1990.
13. R. J. Luebbers, F. Hunsberger, K. S. Kunz, "A Frequency-dependent FDTD formulation for transient propagation in plasma," *IEEE Trans. on Antennas and Propagation*, Vol. 39, pp. 29-39, Jan. 1991.
14. D. M. Sullivan, "A frequency dependent FDTD method for biological applications," *IEEE Trans. on MTT*, Vol. 40, pp. 532-539, Mar. 1992.
15. T. Kashiwa, I. Fukai, "A treatment by FDTD method of dispersive characteristics associated with electronic polarization," *Microwave and Optical Technology Letters*, Vol. 3, pp. 203-205, 1990.
16. R. W. Ziolkowski, N. Engheta *Metamaterials: Physics and Engineering Explorations*, Edited by N. Engheta, IEEE Press, 2006.
17. S. D. Gedney, "An anisotropic pml absorbing media for the fdtd simulation of fields in lossy and dispersive media," *Electromagnetics*, Vol. 16, pp. 399-415, 1996.
18. D. M. Sullivan, "Frequency-dependent FDTD methods using z transforms," *IEEE Trans. on AP*, Vol. 40, pp. 1223-1230, Oct. 1992.